ELSEVIER

Journal of Photochemistry and Photobiology A: Chemistry 112 (1998) 97–102

Journal of Photochemistry and Photobiology A:Chemistry

The photochemical reaction between chlorine and chlorine perchlorate at 366 nm

M.I. López [1], A.E. Croce, J.E. Sicre *

Instituto de Investigaciones Fisicoquímicas Teóricas y Aplicadas (INIFTA), Departamento de Química, Facultad de Ciencias Exactas, Universidad Nacional de La Plata, Casilla de Correo 16, Sucursal 4, La Plata 1900, Argentina

Abstract

The photolysis of Cl_2 in the presence of Cl_2O_4 at 366 nm in the gaseous phase has been investigated at 303 K. The UV absorbance of the gas mixture has been recorded spectrophotometrically after each photolysis interval to monitor the reactant Cl_2O_4 pressure and determine quantitatively the chlorinated reaction products. A quantum yield for Cl_2O_4 consumption of 2.0 ± 0.2 has been determined. The main reaction products are Cl_2O_7, Cl_2 and O_2, accompanied by small quantities of Cl_2O_6 and OClO. A mechanism involving ClO_4 radicals formed in the Cl atom abstraction from Cl_2O_4 by Cl is proposed.

Keywords: Photochemical reaction; Chlorine; Chlorine perchlorate

1. Introduction

The chemistry and photochemistry of the earth's atmosphere have received a great deal of interest during the last years. In particular, the chemistry of the oxides of the halogens, and especially of the chlorine oxides, deserved extensive attention, as these last compounds have been invoked to play an important role in the catalytic loss processes for stratospheric ozone [1,2].

Chlorine oxides may be classified in monochlor- and dichloroxi-derivatives. All these compounds are thermally unstable and may decompose explosively. Along the ClO_x series, only chlorine dioxide, OClO, is stable under certain conditions [3]. On the contrary, ClO and sym-ClO_3 may undergo fast self-association and disproportion [2]. The gas phase self-association of ClO_3 at room temperature leads almost exclusively to chlorine hexoxide, Cl_2O_6 (O_2ClO-ClO_3), as it has been determined not only by infrared spectrophotometry [4] but also by chemical analysis [5].

The last member of the series, sym-ClO_4, has been proposed as an intermediate in the mechanisms of the thermal decompositions of Cl_2O_6 [4–6] and of chlorine heptoxide, Cl_2O_7 [7], but has not been directly identified in the gas phase to date. Only recently, this species has been spectroscopically identified in the matrix isolation of the products of the vacuum thermolysis of Cl_2O_6 [8]. On the other hand, the vacuum thermolysis of Cl_2O_4 ($ClOClO_3$) leads to the formation of ClO and ClO_3 [9]. Ab initio theoretical calculations have been performed [10] to interpret the structure and properties of the chlorine tetroxide radical.

It is well known that chlorine atoms readily abstract chlorine from ClOCl and ClOOCl, leading to ClO and ClOO, respectively [1,2]. Similarly, chlorine atoms are likely to react with chlorine perchlorate, $Cl + ClOClO_3 \rightarrow Cl_2 + ClO_4$. This last process most probably takes a relevant part in the photolysis of Cl_2 in the presence of Cl_2O_4 at 366 nm in the gaseous phase. As a consequence, the photochemical reaction is expected to occur through a mechanism involving ClO_4 radicals. To elucidate this mechanism, the present investigation has been undertaken.

2. Experimental details

The reaction was studied by applying the continuous photolysis method. Most of the experiments were performed in a portable quartz cell, 3 cm long and 4 cm outer diameter, which could be joined to a Bodenstein quartz spiral manometer used as a null instrument in connection with a mercury manometer. A U-trap connected the cell to a standard Pyrex vacuum line used for gas handling. The vessel could be separated from the vacuum line and manometer to be brought to a Cary 14 spectrophotometer. This allowed the reaction mixture to be photolysed and subsequently analysed spectropho-

* Corresponding author.

[1] Deceased.

1010-6030/98/$19.00
PII S1010-6030(97)00276-1

tometrically. The cell was surrounded by a copper tube through which water from a thermostatic bath was circulated, and its temperature maintained at 303 ± 0.05 K by means of a Lauda electronic regulator.

A few experiments were performed in a cylindrical quartz cell 5 cm long and 5 cm outer diameter, connected to the manometers and to the vacuum line, and placed into the thermostatic bath.

The 366-nm line from a high-pressure mercury arc lamp (HBO 200 W) was isolated by means of a Bausch & Lomb grating monochromator ($\Delta\lambda = 19$ nm at 366 nm) and successively focused and collimated before reaching the front window of the reaction cell employing appropriate quartz lenses. The intensity of the light incident on the cell was measured periodically by means of the potassium ferrioxalate actinometer [11].

The reaction mixture consisted typically of about 55 Torr Cl_2 and of 8–22 Torr Cl_2O_4, and was photolyzed at 366 nm during successive intervals of 4–10 min to complete about 1 h. After each interval, the UV absorbance of the gas mixture was recorded using the spectrophotometer to determine quantitatively the chlorinated reaction products. These operations lasted up to 10 min, after which the mixture was further photolysed.

Preliminary experiments showed that no thermal reaction between Cl_2 and Cl_2O_4 takes place in the conditions of the present experiments. However, the spectrophotometric analysis of the reaction mixture prior to photolysis always revealed a small amount of OClO between 0.1 and 0.4 Torr. This observation agrees with those made in previous investigations [12].

Chlorine dioxide, chlorine, oxygen and argon were obtained and purified as it has been previously described [3,5].

Chlorine perchlorate was obtained by the 436-nm photolysis of chlorine dioxide [12] employing the last cell described above.

3. Results

The experiments carried out to establish the reaction stoichiometry showed that the 366-nm photolysis of Cl_2 in the presence of Cl_2O_4 proceeds with an increase of total pressure. The photolysis of 54.1 Torr Cl_2 in the presence of 21.9 Torr Cl_2O_4 was performed during 210 min with a total pressure change of 14.8 Torr, and during additional 30 min without any subsequent pressure change. After this, a volatile fraction of 15.4 Torr in O_2 was separated from the reaction mixture by distillation at the liquid nitrogen temperature. Further distillation at 173 K of the residue allowed the separation of 67.3 Torr of Cl_2, which was identified by UV–visible spectrophotometry. The infrared spectrum of the fraction condensed at 173 K (8.1 Torr) showed the characteristic absorption bands of dichlorine heptoxide [13].

The ratio of the amounts of Cl_2O_4 to Cl_2O_7 to Cl_2 to O_2 of 3:1.1:1.8:2.1 clearly indicates that, within the limits of the experimental errors, the reaction stoichiometry is given by

$$2Cl_2O_4 \rightarrow Cl_2O_7 + 1/2O_2 + Cl_2$$

together with

$$Cl_2O_4 \rightarrow 2O_2 + Cl_2$$

In experiments in which the photolysis was interrupted in the way described in Section 2, besides Cl_2, Cl_2O_4, Cl_2O_7 and a small amount of OClO, the intermediate stable product Cl_2O_6 could also be determined. The UV spectra of Cl_2O_4 [12], Cl_2O_6 [5], Cl_2 [14,15] and Cl_2O_7 [16] are depicted in Fig. 1. As it has been pointed out [17], being the whole set of absorption coefficients well-known and assuming the additivity of the absorbances of the single components, the application of Lambert–Beer law allows the calculation of the pressure of each of them on an empirical basis. First, Cl_2O_4, Cl_2O_6 and Cl_2O_7 are the only components of the reaction mixture that absorb between 210 and about 260 nm. To

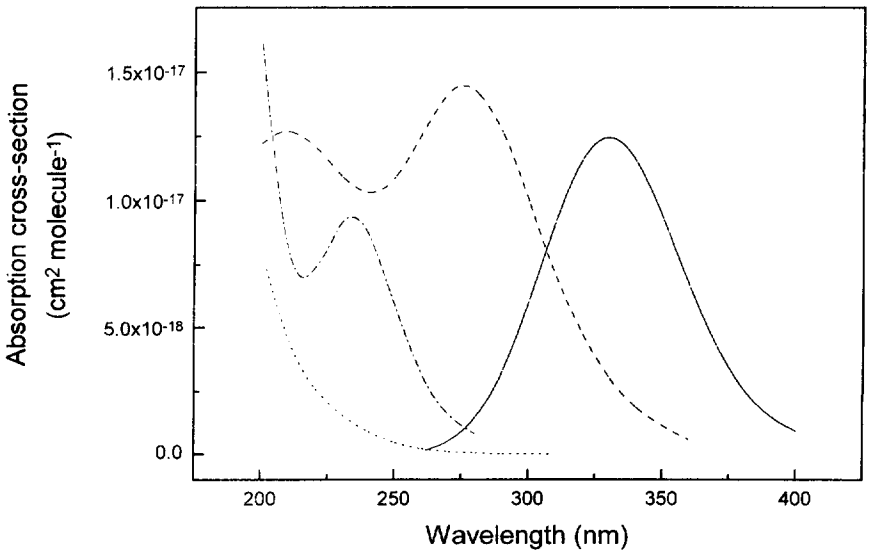

Fig. 1. Absorption cross-sections for Cl_2O_6 (- - -), $Cl_2O_4 \times 10$ (– · –), $Cl_2O_7 \times 25$ (· · ·) and $Cl_2 \times 50$ (———), as a function of wavelength.

minimize the delay between the successive photolysis periods, only three wavelengths within this range, namely, 210, 230 and 250 nm were selected for the determination of these components. The absorption coefficients for Cl_2O_4, Cl_2O_6 and Cl_2O_7 fitted from the spectrophotometric determinations at the three wavelengths given in Table 1 are in good agreement with those reported. On the other hand, calibrated absorption spectra of Cl_2/OClO mixtures in the region 280–450 nm, allowed the correction by OClO of the total absorption measured at 340 nm. Once Cl_2O_6 has been determined, the absorbance of this compound at 340 nm is calculated, then subtracted from the absorption corrected by OClO to obtain the amount of Cl_2.

In a typical set of experiments, the pressure of each reactant, Cl_2 and Cl_2O_4, was measured in the portable cell and the initial UV–visible spectrum recorded. In this way, the initial composition of the reaction mixture was established. The cell filled with the gas mixture was then exposed to the 366-nm light during a given time interval, after which the total absorbance was recorded between 300 and 400 nm and at the four fixed wavelengths of 210, 230, 250 and 340 nm. The pressure results for Cl_2O_4, Cl_2, Cl_2O_6 and Cl_2O_7 calculated from the spectrophotometric information are given in Table 2 as a function of the time of photolysis for the three sets of experiments. The pressure of Cl_2O_4 decreases linearly over almost the whole time range, while Cl_2O_6 and Cl_2O_7 pressures start from zero and increase as a function of time. Cl_2O_6 reaches a maximum pressure towards the time when Cl_2O_4 is almost totally consumed, and finally decays to zero. As for Cl_2, the difference between the determination at 340 nm corrected by the absorptions of Cl_2O_6 and of OClO at this wavelength, and the initial pressure of Cl_2, yields the amount of this compound formed in a given time interval, subject to a relatively high average error as shown in Table 2. The set of experiments no. 2 have been performed in the presence of 402.9 Torr of the added gas Ar. Although an initial amount of OClO of 0.35 Torr was determined for set no. 3, the pressure of OClO after each photolysis period never exceeded about 0.20 Torr. The analytical method employed here does not allow to discriminate a contribution of the photochemical reaction to OClO pressure from the amount of OClO formed during the dark periods. The Cl_2O_4, Cl_2O_6 and Cl_2O_7 pressures for the set of experiments no. 3 are also represented as a function of time in Fig. 2.

The quantum yield for Cl_2O_4 consumption can be calculated as $\Phi = \Delta(Cl_2O_4)/(I_{abs}\Delta t)$, where $\Delta(Cl_2O_4)$ indicates the amount of Cl_2O_4 consumed during a given photolysis time interval, Δt. I_{abs} denotes the intensity of the light absorbed by Cl_2, calculated as $I_{abs} = f_{abs}I_0$, where I_0 is the measured light intensity at 366 nm. The fraction of light absorbed by Cl_2 at 366 nm, f_{abs}, has been calculated employ-

Table 1
Absorption coefficients (in $Torr^{-1}\ cm^{-1}$) for Cl_2O_4, Cl_2O_6 and Cl_2O_7 at the three wavelengths employed for the spectrophotometric determinations

λ (nm)	$\varepsilon(Cl_2O_4)$	$\varepsilon(Cl_2O_6)$	$\varepsilon(Cl_2O_7)$
210	0.0290	0.538	0.0704
230	0.0381	0.441	0.0244
250	0.0254	0.436	0.0067

Table 2
Experimental Cl_2O_4, Cl_2O_6, and Cl_2O_7 pressures (Torr) as a function of time

Set of experiments	Time (min)	Cl_2O_4	Cl_2O_6	Cl_2O_7	Cl_2	OClO
1	0	11.3	–	–	53.6	0.10
	10	10.0	0.42	0.48	52.3	
	20	7.5	0.61	1.2	54.3	
	30	5.0	0.75	1.8	55.8	
	40	2.9	0.79	2.4		
	50	0.95	0.80	3.1		
	60	0.27	0.24	4.0		
	70	–	–	3.9		
2	0	7.7	–	–	57.8	0.10
	10	7.9	0.16	0.49	59.3	
	20	5.7	0.33	0.98	60.3	
	30	3.1	0.51	1.2	60.9	
	40	1.1	0.56	1.9	62.6	
	50	–	0.078	2.2	60.8	
	60	–	–	2.3	60.5	
3	0	16.9	–	–	51.6	0.35
	4	16.6	0.39	0.40	52.5	0.23
	8	14.4	0.57	1.20	54.3	0.17
	12	13.0	0.69	1.24	55.5	0.25
	16	11.9	0.76	1.23	57.1	0.22
	20	8.35	0.95	2.52	57.3	0.17
	24	5.95	1.08	2.88	57.2	0.18
	28	3.81	1.14	3.56	58.2	0.20
	32	3.04	1.07	4.41	59.8	0.16
	36	1.84	1.12	4.83	60.3	0.15
	40	0.52	0.41	5.55	59.6	0.05
	44	–	0.011	5.72	58.2	–
	48	–	–	5.71	58.9	–

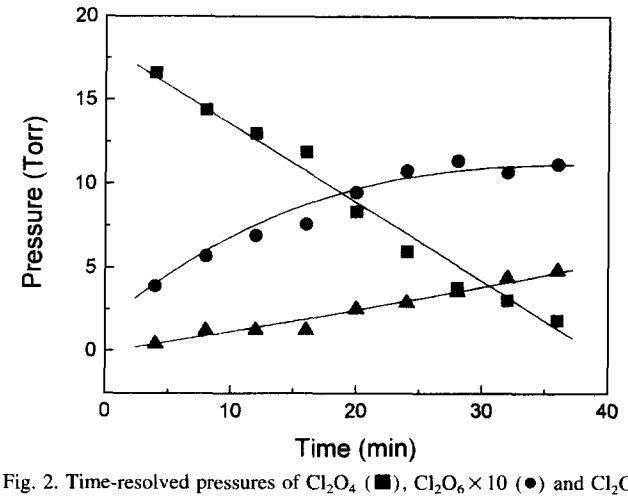

Fig. 2. Time-resolved pressures of Cl_2O_4 (■), $Cl_2O_6 \times 10$ (●) and Cl_2O_7 (▲). The solid lines represent the pressures calculated employing the rate constants in Table 4.

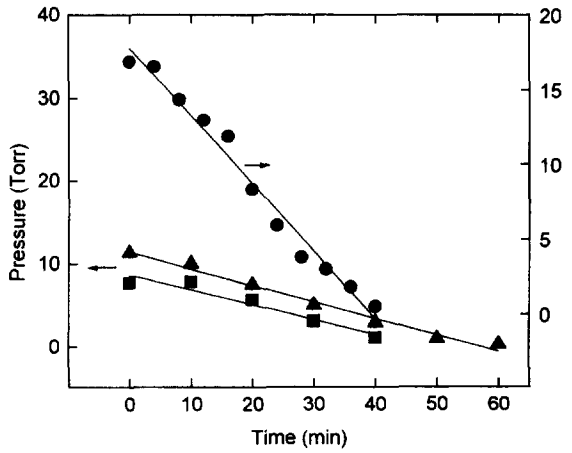

Fig. 3. Time dependence of Cl_2O_4 pressure. The straight lines correspond to the linear regression of the results from the three sets of experiments: (▲) no. 1, (■) no. 2 and (●) no. 3.

Table 3
Quantum efficiency for Cl_2O_4 consumption (Φ)

Set of experiments	Cl_2 (Torr)	f_{abs}	I_0 (Torr min^{-1})	Slope (Torr min^{-1})	Φ
1	54.0	0.42	0.23	−0.20	2.1
2	60.8	0.45	0.21	−0.18	1.9
3	56.9	0.43	0.56	−0.45	1.9

ing the Lambert–Beer law with the average Cl_2 pressure, the optical path length of the cell, $l=3$ cm, and the absorption coefficient for Cl_2 at 366 nm, $\varepsilon(Cl_2)=1.44\times10^{-3}$ $Torr^{-1}$ cm^{-1}. Fig. 3 shows the linear dependence of Cl_2O_4 pressure on time for the three sets of experiments. The slope of the straight lines, the input data f_{abs} and I_0, as well as the resulting Φ values, are shown in Table 3. An experimental average quantum yield for Cl_2O_4 consumption of 2.0 ± 0.2 has been obtained from the results for the three sets of experiments.

At the photolysis wavelength, two of the reaction products, namely Cl_2O_6 and OClO, absorb light. Therefore, it is necessary to know to what extent this fact affects the fraction of the light intensity absorbed by Cl_2, and which are the products of the secondary photolysis. The scarce amount of OClO present during the experiments renders unimportant the influence of this substance. On the other hand, the maximum pressure of Cl_2O_6 determined in an experiment is approximately 1 Torr, consequently at a pressure of Cl_2 equal to 60 Torr, and the ratio of the absorbances at 366 nm for Cl_2O_6 to Cl_2 is 0.065 at the most. This affects the fraction of the light intensity absorbed by Cl_2 within the limits of ±10% found for the experimental error. It has been pointed out that the product Cl_2O_6 is transformed to Cl_2O_4 by thermal decomposition [5] and, at least in a matrix, also by photolysis [4].

4. Discussion

The experimental results have been interpreted by means of the mechanism that will be described in the following. A numerical simulation based on the Runge–Kutta algorithm has been applied to fit the time evolution of the concentrations of reactants and products.

The reaction begins with chlorine photodissociation [1]

$$Cl_2+h\nu(\lambda=366\ nm)\rightarrow 2Cl \quad (1)$$

followed by the reaction

$$Cl+ClOClO_3\rightarrow Cl_2+ClO_4 \quad (2)$$

High rate coefficient values for other chlorine abstraction reactions by chlorine atoms, $Cl+ClOR\rightarrow Cl_2+RO$ ($R=FSO_2$ [18], H [19], CH_3 [19,20], *tert*-C_4H_9 [19], FCO [21]) have been recently reported. On the other hand, in the presence of OClO the fast bimolecular reaction: $Cl+OClO\rightarrow 2ClO$ [1], also occurs. However, the rate of this last reaction should be much lower than that of reaction (2) under our experimental conditions.

Subsequently, the self-reaction of the ClO_4 radicals

$$ClO_4+ClO_4\rightarrow 2ClO_3+O_2 \quad (3)$$

and

$$ClO_4+ClO_3\rightarrow Cl_2O_7 \quad (4)$$

interpret the occurrence of Cl_2O_7 as a main reaction product. The ClO_3 radicals may undergo the recombination reaction $ClO_3+ClO_3\rightarrow Cl_2O_6$, for which a rate constant of the same order of magnitude as k_4 is expected [22]. However, reaction (4) is fast enough under the conditions of the present experiments, and consequently, the only fate for the ClO_3 radicals.

The formation of the relatively large amount of chlorine, besides of that produced through reaction (2), may be adequately accounted for by

$$ClO_4+ClO_4\rightarrow Cl_2+4O_2 \quad (5)$$

in spite of the fact that the mechanism of this reaction is a matter to discuss.

The set of reactions (1)–(5) lead to the rate equation $-d[Cl_2O_4]/dt=2I_{abs}$ from which a quantum efficiency for Cl_2O_4 decomposition of 2 can be calculated. Therefore, the mechanism allows an interpretation of the average quantum yield of 2.0 ± 0.2 for Cl_2O_4 obtained from the experimental results.

To account for the fact that Cl_2O_6 is formed to a larger extent at the beginning of each set of experiments when Cl_2O_4 pressures are higher, the exothermic reaction

$$ClO_4+Cl_2O_4\rightarrow Cl_2O_6+OClO \quad (6)$$

may occur followed by

$$ClO_4+OClO\rightarrow Cl_2O_6 \quad (7)$$

On the other hand, the thermal decomposition of Cl_2O_6, which leads to the formation of Cl_2O_4 and O_2 through a first-

order kinetics [5], and much less the photolysis of Cl_2O_6 at 366 nm sensitized by chlorine [23,24], contribute to Cl_2O_6 depletion.

A mechanism for the thermal decomposition of Cl_2O_6 including the dissociation reaction

$$Cl_2O_6 \rightarrow ClO_4 + OClO \qquad (-7)$$

has been recently proposed on thermodynamic grounds [25]. This reaction may be followed by the exothermic process (López and Sicre, to be published).

$$ClO_4 + OClO \rightarrow Cl_2O_4 + O_2 \qquad (8)$$

The complex reaction between two ClO_4 radicals

$$ClO_4 + ClO_4 \rightarrow 2OClO + 2O_2 \qquad (9)$$

accounts for the fact that Cl_2O_6 is still formed when small amounts of Cl_2O_4 are present as seen in Fig. 2.

If reactions (6), (7), (−7), (8) and (9), are included in the mechanism besides reactions (1)–(5), the following reaction rate equation

$$-d[Cl_2O_4]/dt = 2I_{abs} + k_6[ClO_4][Cl_2O_4] - k_8[ClO_4][OClO]$$

results. The average experimental quantum efficiency of 2.0 ± 0.2 leads to the conclusion that the two last terms on the right-hand side member of the preceding equation balance each other along a given series of experiments.

The simulation employing reactions (1)–(7), (−7), (8) and (9) allows to draw the solid lines in Fig. 2 for the set of experiments no. 3. Table 4 shows the input data for the respective rate constants. The rate constants k_3, k_5, k_6, k_8 and k_9 were obtained by numerical fitting of the experimental results from Table 2, for the times before the reactant Cl_2O_4 is completely consumed. Due to the fact that reaction (2) is the only outcome for Cl atoms, the numerical fitting does not depend on the value of this rate constant. The mechanism for Cl_2O_6 thermal decomposition given by reactions (3)–(7), (−7), (8) and (9) [24], different from those proposed in Ref. [5], and the experimental rate constant $k_{exp} = 0.0209\ min^{-1}$ [5], allow to calculate k_8 as $k_{exp} \cong K_{-7}k_8$, where K_{-7} is the equilibrium constant for Cl_2O_6 decomposition into ClO_4 and OClO. The scarce photochemical decomposition of Cl_2O_6, as well as the thermal decomposition of Cl_2O_6 during the dark periods within which the spectrophotometric measurements are performed, contribute to obtain a slightly higher value for k_8 by numerical fitting. Consequently, different k_8 values result for the three sets of experiments as shown in Table 3. The value for K_{-7} from Ref. [25] has been used in the calculations, and the numerical fitting is practically independent of the individual values of k_7 and k_{-7}. Therefore, a value for k_7, a factor of at least 200 higher than k_8, has been fixed.

From the simulation, a stationary pressure of about 0.05 Torr for ClO_4 radicals results. Although this conclusion arises from calculations based on indirect evidences, the potential use of this system as source of ClO_4 through the reaction of chlorine atoms with chlorine perchlorate deserves further attention. Time-resolved experiments in which shortlived intermediate species are monitored would offer a more conclusive answer and are foreseen.

Table 4
Rate constants and reaction enthalpies for the reactions included in the mechanism

Reaction	ΔH (kcal mol^{-1}) [a]	Rate constants [b]
(3) $ClO_4 + ClO_4 \rightarrow 2ClO_3 + O_2$	−0.4	3.8×10^{1}
(5) $ClO_4 + ClO_4 \rightarrow Cl_2 + 4O_2$	−100.0	3.5×10^{1}
(6) $ClO_4 + Cl_2O_4 \rightarrow Cl_2O_6 + OClO$	−12.1	3.1×10^{-2}
(7) $ClO_4 + OClO \rightarrow Cl_2O_6$	−20.9	1.5×10^{5}
(−7) $Cl_2O_6 \rightarrow ClO_4 + OClO$	20.9	8.1 [c]
(8) $ClO_4 + OClO \rightarrow Cl_2O_4 + O_2$	−35.8	5.0×10^{2} [d]
		5.5×10^{2} [e]
		7.9×10^{2} [f]
(9) $ClO_4 + ClO_4 \rightarrow 2OClO + 2O_2$	−54.0	1.2×10^{1}

[a] Data from Ref. [25].
[b] Torr^{-1} min^{-1} unless indicated otherwise.
[c] Min^{-1}.
[d] For set of experiments no. 1.
[e] For set of experiments no. 2.
[f] For set of experiments no. 3.

Acknowledgements

This research project was supported by the Consejo Nacional de Investigaciones Científicas y Técnicas, the Comisión de Investigaciones Científicas de la Provincia de Buenos Aires and the Universidad Nacional de La Plata. Helpful discussions with Dr. Enrique Castellano are gratefully acknowledged.

References

[1] W.B. DeMore, S.P. Sander, C.J. Howard, A.R. Ravishankara, D.M. Golden, C.E. Kolb, R.F. Hampson, M.J. Kurylo, M.J. Molina, Chemical Kinetics and Photochemical Data for Use in Stratospheric Modeling, JPL Publication 94-26, 1994.
[2] R.P. Wayne, Atmos. Environ. 29 (1995) 2675.
[3] M.I. López, A.E. Croce, J.E. Sicre, J. Chem. Soc., Faraday Trans. 90 (1994) 3391.
[4] M. Jansen, G. Schatte, K.M. Tobias, H. Willner, Inorg. Chem. 27 (1988) 1703.
[5] M.I. López, J.E. Sicre, J. Phys. Chem. 94 (1990) 3860.
[6] A.J. Arvia, W.H. Basualdo, H.J. Schumacher, Z. Anorg. Allg. Chem. 286 (1956) 58.
[7] R.V. Figini, E. Coloccia, H.J. Schumacher, Z. Phys. Chem. 14 (1958) 32.
[8] H. Grothe, H. Willner, Angew. Chem., Int. Ed. Engl. 35 (1996) 768.
[9] H. Grothe, H. Willner, Angew. Chem., Int. Ed. Engl. 33 (1994) 1482.
[10] T.J. Van Huis, H.F. III Schaeffer, J. Chem. Phys. 106 (1997) 4028.
[11] C.G. Hatchard, C.A. Parker, Proc. R. Soc. London, Ser. A 235 (1956) 518.

[12] M.I. López, J.E. Sicre, J. Phys. Chem. 92 (1988) 563.
[13] J.D. Witt, R.M. Hammaker, J. Chem. Phys. 58 (1973) 303.
[14] D. Maric, J.P. Burrows, R. Mellor, G.K. Moortgat, J. Photochem. Photobiol. A Chem. 70 (1993) 205.
[15] S. Hubinger, J.B. Nee, J. Photochem. Photobiol. A Chem. 86 (1995) 1.
[16] C.L. Lin, J. Chem. Eng. Data 21 (1976) 411.
[17] H. Mark, Appl. Spectrosc. 42 (1988) 1427.
[18] A.E. Croce, C.J. Cobos, E. Castellano, Chem. Phys. Lett. 158 (1989) 157.
[19] A. Kukui, J. Roggenbuck, R.N. Schindler, Ber. Bunsenges. Phys. Chem. 101 (1997) 281.
[20] S.A. Carl, C.M. Roehl, R. Müller, G.K. Moorgat, J.N. Crowley, J. Chem. Phys. 100 (1996) 17191.
[21] A.E. Croce, C.J. Cobos, E. Castellano, Chem. Phys. Lett. 266 (1997) 253.
[22] C.J. Cobos, J. Troe, J. Chem. Phys. 83 (1985) 1010.
[23] A.C. Burns, G.K. Rollefson, J. Am. Chem. Soc. 56 (1934) 2245.
[24] M.H. Kalina, J.W.T. Spinks, Can. J. Res. B 16 (1938) 382.
[25] A.J. Colussi, M.A. Grela, J. Phys. Chem. 97 (1993) 3775.